Fermi National Accelerator Laboratory

FERMILAB-Pub-87/183-E
[E-741/CDF]

The CDF Vertex Time Projection Chamber System*

F. Snider
University of Chicago
Chicago, Illinois 60637, USA

M. Binkley, J. Huth, R. Kephart, C. Newman-Holmes, S. Palanque*,
J. Patrick, R. Yarema, G. P. Yeh, and T. Zimmerman
Fermi National Accelerator Laboratory†
P.O. Box 500, Batavia, Illinois 60510, USA

M. Schub
Purdue University
West Lafayette, Indiana 47907, USA

F. Abe‡, K. Kondo, T. Mimashi, and M. Sekiguchi
Institute of Physics, University of Tsukuba
Sakura, Niihari, Ibaraki 305, Japan

July-August 1987

*Submitted to Nucl. Instrum. Methods A

The CDF Vertex Time Projection Chamber System

F. Snider

University of Chicago

Chicago, Illinois 60637,USA

M. Binkley, J. Huth, R. Kephart, C.Newman-Holmes, S. Palanque *

J. Patrick, R. Yarema, G.P. Yeh, and T. Zimmerman

Fermi National Accelerator Laboratory†

Batavia, Illinois 60510, USA

M. Schub

Purdue University

W. Layfayette, IN, 47907

F. Abe ‡, K. Kondo, T. Mimashi, M. Sekiguchi

Institute of Physics, University of Tsukuba

Sakura, Niihari, Ibaraki 305, Japan

June 12, 1987

Abstract

The Vertex Time Projection Chamber (VTPC) system is one of the major components of the charged particle tracking system for the Collider Detector at Fermilab (CDF). The chambers cover about seven units of pseudo-rapidity (η)and must be capable of handling substantially more than the 30-35 charged particle tracks produced by typical $\bar{p}p$ collisions at CM energies of 1.8 TeV. The chambers are optimised to provide the good

*on leave from CEN Saclay DPdPE - STIPE

†Operated by Universities Research Association under Contract with the U.S. Department of Energy No. DE-AC02-76CH03000

‡National Lab. for High Energy Phys., KEK , Oho-machi, Tsukuba-gun, Ibaraki-ken, 305, Japan

pattern recognition in the r-z view required to locate the event vertex, measure the overall event topology, and to complement the r-ϕ tracking in the large axial wire drift chamber that surrounds them. The chambers provide r-z information using TDC data from sense wire signals. Information on the ϕ of tracks is obtained from cathode pad signals on a subset of chambers read out by a FADC system. A similar system measures dE/dx of tracks in the forward cones surrounding the exiting beams. Because of the large number of photons that pass through the detector during each collision, novel techniques are required to reduce the amount of material in the chamber. These techniques include a custom surface mount integrated circuit preamplifier, epoxy-graphite and Kapton covered foam structural members, and miniature coaxial signal cables. The mechanical construction of the chamber, radiation length vs angle, and details of the electronics are described. The event reconstruction, corrections, and preliminary performance results for 1.8 TeV $\overline{p}p$ collisions are also discussed.

1 Design Requirements

The VTPC (Vertex Time Projection Chamber) system consists of eight double time projection chambers surrounding the beam pipe and mounted end-to-end along the beam direction (z-axis). The location of the VTPC in the CDF central detector [1] is shown in Figure 1. The VTPC contributes both stand-alone tracking and measurements which complement those obtained with the Central Tracking Chamber (CTC) [2] and the Forward Tracking Chambers (FTC)[3].

The basic design requirements of the VTPC system were:

1. Provide z-vertex determination. The distribution of event vertices at the Tevatron collider is a Gaussian along the beam axis with a typical FWHM of 75 cm. Knowledge of the location of the event vertex is a first order correction in the

calculation of physics quantities such as the transverse energy and is the starting point for offline event reconstruction.

2. Determine overall event topologies over a very wide range in polar angles ($3.5° < \theta < 176.5°$), and perform various charged particle measurements such as $< N_{ch} >_{TOTAL}$ and $dN_{ch}/d\eta$ for $-3.5 < \eta < 3.5$.

3. Identify multiple interactions in the same beam crossing. When the Tevatron is operated in three bunch mode at a luminosity of $10^{30}\text{cm}^{-2}\text{s}^{-1}$ at least one event in five will contain a multiple interaction. This requires good pattern recognition in the r-z plane in events often containing a hundred or more charged particle tracks.

4. Detect charged particle tracks near the vertex where the amount of material traversed is still small. This is important in order to minimize photon conversion contamination of electrons.

5. Provide intermediate angle tracking ($10° < \theta < 30°$) . In this angular region VTPC information is used in conjunction with limited CTC information to provide both pointing and momentum measurements. This is essential for $e/\pi°$ separation in the endplug calorimetry.

6. Provide forward angle tracking ($3.5° < \theta < 10°$). The VTPC wire information must provide pointing in the r-z projection for the forward calorimetry. Similarly, the pad r-ϕ reconstruction can be used in conjunction with FTC information to determine the sign of the charge of forward particles, particularly leptons. In addition, a rough momentum measurement is possible for low momentum particles in this region.

7. Finally, to minimize the effects on other tracking systems from secondary interactions and multiple scattering, the entire VTPC system must be very thin in terms of radiation lengths.

2 Chamber Design

Each of the eight octagonal VTPC modules has a central high voltage grid that divides it into two 15.25 cm long drift regions. It is eventually planned to operate the Tevatron in six bunch mode with 3.5 μs between crossings. The 15.25 cm drift length is chosen so that the maximum drift time is less than 3.5 μs when the drift velocity in the gas is 46 μm/ns (*eg.* argon-ethane 50/50 at atmospheric pressure and E=320 V/cm). The electrons drift away from the center grid until they pass through a cathode grid and enter one of the two proportional chamber endcaps. Each endcap is divided into octants, with 24 sense wires and 24 cathode pads in each octant. The arrival times of the electrons at the sense wires give a picture of the event in the r-z plane. In addition the sense wires and pads in some endcaps are instrumented with an analog pulse height readout using Flash Analog to Digital Converters (FADC), so that dE/dx and ϕ information is available for particles produced at angles between 5° and 25° with respect to each beam axis. Two VTPC modules are shown in Figure 2. Adjacent modules have a relative rotation angle of $\phi_\circ = \arctan(.2)$ about the beam axis. For tracks passing through at least two modules, this eliminates inefficiencies near octant boundaries and provides ϕ information from small angle stereo.

As viewed from the drift region, an octant consists of a cathode grid followed by a plane of field shaping wires, a plane of sense wires, and a resistive ink cathode

plane. Three rows of pads are located behind the resistive cathode, separated by 150 μm of epoxy-fiberglass (G-10). A pad covers 4.12 cm in radius and 1.4 cm in r-ϕ. The sense wire plane is 1 cm from both the cathode grid and resistive cathode, and the plane of field shaping wires is offset by 3 mm toward the cathode grid from the sense wire plane. The spacing between both field shaping wires and sense wires is 6.34 mm. The field shaping wires are offset by 1/2 wire spacing in r with respect to the sense wires. Since the sense wires in each octant are read out separately, the wires in adjacent octants are offset radially by 1/2 wire spacing. The active area of the chamber extends from about $r = 7$ cm to $r = 21$ cm. A more detailed view of the proportional chamber portion of the VTPC is shown in Figure 3. Figure 4 is a photograph of four VTPC modules in their service position during installation. A summary of VTPC parameters is given in Table 1.

3 Low-mass Construction

An average of $\sim$ 30 photons pass through the VTPC per event. Since the VTPC is located inside the CDF central and forward tracking chambers, it is extremely important to minimize the effective thickness of the chamber in radiation lengths. Any photon conversions which do occur in the VTPC can result in large local track density in these systems and can make pattern recognition and track reconstruction difficult or impossible. In addition, such conversions degrade the electron identification capability of the experiment and the multiple Coulomb scattering adversely affects the CTC momentum resolution. As a result the materials used in constructing the VTPC were chosen with particular emphasis toward low mass and long radiation

length. The mechanical structure of the VTPC consists mainly of such light-nuclei materials as Rohacell foam [4], Kapton film [5], and epoxy-fiber laminates employing either glass or graphite fibers. The basic technique is to use a core of lightweight foam covered with a strong skin. This construction puts the denser material where it contributes most to the moment of inertia and therefore provides the best stiffness-to-mass ratio. The use of graphite fibers is particularly effective since they have excellent strength, a high modulus, and a long radiation length.

The VTPC field cage assembly consists of a high voltage center grid and two cathode grids supported by four octagonal epoxy-graphite/foam frames. These frames are attached to the walls of the VTPC field cage and provide a lightweight but stiff base for the field cage structure. The field cage walls are constructed of a three-layer Kapton-foam-Kapton lamination that supports the field shaping electrodes. The electrodes are overlapping copper strips etched on both sides of the inner copper clad Kapton skin. The Kapton is 25 μm thick, the cladding is 16 μm of copper, and the foam is 2 mm thick. Construction of the field cage begins by prefabrication of the field cage walls. The outer field cage is octagonal in shape, the inner wall is cylindrical. The octagonal epoxy-graphite/foam frames are also prefabricated by laying up a two layer laminate of 140 μm graphite fibers impregnated with a B-stage epoxy [6] around a foam core and curing this assembly in a precision mold at 150° C for five hours. The cathode grids are made of stainless steel screen with 50 μm wires on 500 μm centers[7]. The central high voltage grid employs screen with 50 μm wires on 1000 μm centers. The screens are stretched on a transfer fixture to a tension of 160 N/m. The field cage walls, frames, and screens are then assembled and glued on a machined alignment jig that controls the screen to screen spacing as

well as the electrode alignment to a precision of 50 μm. After assembly the transfer fixture is removed and the epoxy-graphite frames then support the screen tension. These frames also prevent the VTPC modules from deforming due to the stresses of the mounting system and the weight of the cables. The precise screen-to-screen spacing is maintained by 1.6 mm dia. "pultruded" glass rods [8] at each corner of the octagonal field cage.

The VTPC endcaps are fabricated with similar techniques. Circuit boards employing 150 μm thick epoxy-fiberglass laminates (G-10) form a sandwich with 3 mm thick foam to provide stiffness for the endcaps. The surface of one circuit board is coated with a resistive polymer ink [9] with a surface resistivity of about 10 MΩ/square. The other side of this board is clad with 13.5 μm of copper. This copper cladding is etched to provide the cathode readout pads. Connections to these pads are made with conductive epoxy using copper strips passing through 6.4 mm diameter holes in the foam to a readout board at the extreme ends of the module. The pad preamplifiers are later mounted directly to this board. After the cathode sandwich is complete, radial readout boards and thin G-10 frames are glued to it in another precision assembly fixture. These radial boards consist of a custom 0.74 mm thick three-layer circuit board. The outer layers of this board are etched to provide electric field shaping electrodes, as well as terminals to which both field shaping and sense wires are soldered. The signals from the sense wires pass through plated-through holes and are carried out radially on traces located in the middle of the circuit board. At the outside radius the traces resurface and connect to the preamplifiers mounted on the radial boards. After etching, the boards are laser machined in a single setup that cuts them to shape and laser drills precision holes that determine

the field shaping and sense wire locations. After the endcap assembly is removed from its fixture, the final steps are to thread, tension and solder the wires and to mount the endcaps to the drift cage. The positional accuracy of the laser machining as well as the accuracy of installed wires was verified using a Cordax [10] machine and was found to be 55 μm RMS.

The same concern for low-mass solutions also prevailed in the choice and design of the chamber-mounted electronics and cables for the VTPC. Extensive use of surface-mount technology on thin (0.625 mm) G-10 boards minimizes the mass contribution of the preamplifiers. The cables used for both wire and pad signals represent the limit of current technology for copper coaxial cables optimized for low mass. Figure 5 shows the average amount of material in radiation lengths which a particle originating at the center of the detector traverses before reaching the active volume of the VTPC (dotted line), after passing through the entire VTPC system (dot-dash line), and before entering the active volume of the CTC or FTC (solid line). The plot is obtained by adding the mass contribution of each detector component weighted by appropriate angular factors. The material in the electronics and cables located on the outer perimeter of the chamber is averaged in azimuth over the polar angles which the component subtends.

The amount of material traversed is lowest over the angular region of full coverage by the CTC ($50° < \theta < 130°$) Over this region a particle on average crosses less than 0.7 % of a radiation length before it is tracked by the VTPC, and less than 3.2 % before entering the CTC. The amount of material traversed before the active volume of the VTPC is 0.5 % of a radiation length at $\theta = 90°$ and is equally divided among the 0.5 mm Be beam pipe, its Faraday cage, and the VTPC inner field cage.

The traversed mass distribution peaks between 10-20° with respect to each exiting beam with 6 % of a radiation length before, and 22 % after tracking by the VTPC in the worst region. However, in this angular range, the VTPC provides nearly all tracking information available. Thus the material after the VTPC active volume has a relatively small impact on other tracking systems. In the angular region covered by the FTC ($2° < \theta < 10°$), the amount of material crossed by a particle passing through the VTPC drops to between 5-10 % of a radiation length. The discontinuities in the plot correspond to places where a new set of cables is added or a new proportional chamber traversed. The drop in effective thickness below 10° is due to the fact that the signal cables exit the gas vessel at 10°, then pass between the CTC endplate and the end plug calorimeter system, away from the path of particles pointing at the FTC. In the current version of the VTPC, copper in cables and laminates contributes a significant fraction of the total radiation length of the overall system. Alternatives such as vapor deposited copper, aluminum laminates and aluminum coaxial cables were explored but thus far have proved unsatisfactory.

4 Electronics

The front end electronics for the VTPC consists of preamplifiers mounted directly on the chambers, amplifier-shaper-discriminator (ASD) cards located on the central detector endwalls, and FASTBUS TDCs and FADCs located in the counting room. The preamplifiers are connected to the ASD cards by 10 m long miniature coaxial cables. Each coax is 0.75 mm in diameter and is contained in a 25 coax ribbon cable custom manufactured for the VTPC system by Junkosha Co. Ltd Japan [11].

The individual coax has an inner conductor with a resistance of 0.5 Ω/m (32 gauge equivalent) and a shield with 0.27 Ω/m. The characteristic impedance is 42 Ω and the rise time for the 10 meter length is about 5 ns (10% to 70%). The signals sent from the ASD cards to the TDCs and FADCs in the counting room are differential. The ECL level signals for the TDCs are sent on a 61 m long flat cable (polyethylene dielectric) with two signal wires and one isolating ground wire per channel[12]. The FADC signals are sent on a round cable with 24 individually shielded twisted pairs surrounded by a collective outer shield[13]. The calibration system designed for the CTC is used to generate test pulses and to monitor the stability of the VTPC electronics [2].

4.1 Wire Electronics

The wire preamplifier is a fast grounded-base amplifier. To minimize mass, the basic circuit is implemented on a custom integrated circuit using analog master slice techniques [14]. The resulting chip (Fujitsu MB43458) contains four preamplifiers on a single substrate in a 14 pin surface mount package. The 24 channel surface mount preamplifier cards for the VTPC use six of these chips [15] and include both protection diodes and a resistor network to cancel opposite sign cross-talk. The ribbon coax cables are soldered directly to the preamplifier card in order to provide a good low inductance ground connection. Power dissipation is an important design consideration due to the difficulty of cooling the centrally located VTPC preamplifiers without adding excessive material. The circuit dissipates about 25 mW per channel.

Each channel on the wire ASD card [2] consists of a pull-down resistor for the preamplifier, an emitter follower, a shaping network, an amplifier, and a LeCroy

MVL407 comparator [16]. The shaping network consists of a pole-zero filter which cancels most of the long $1/t$ tail of the signal (RC about 700 ns) and a short time constant integrator (RC about 30 ns) which widens the time window over which the fast signals from different electrons are added. Computer simulations indicate that the integration improves the resolution and reduces the number of excursions below the comparator threshold for tracks at small angles with respect to the beams. The comparator produces a time-over-threshold ECL logic signal that is sent to the TDC. The TDCs are LeCroy 1879 FASTBUS modules with multihit capabilities. There are 512 time bins in the TDC, each time bin corresponding to about 320 μm. The TDCs are read out using a modified version of the SLAC Scanner Processor (SSP) [17]. The average event taken with minimum trigger bias contains 8 kbytes of TDC data. A schematic of this system is presented in Figure 6.

4.2 Pad Electronics

A simplified schematic of the VTPC pad electronics is shown in Figure 7. The pad preamplifiers are LeCroy HQV802 hybrid FET input charge sensitive amplifiers custom packaged for the VTPC system with eight channels in a low mass plastic case. These packages combine low mass (3.5 grams for eight channels), low power consumption (about 60 mW per channel for our conditions), and low noise (about 1500 electrons equivalent for a 200 ns integration time). The hybrids are mounted on a thin 24 channel circuit board containing protection diodes and a series back termination resistor for each channel.

Each channel of the pad-amplifier-shaper (PAS) card has a pull-down resistor for the preamplifier, a pole-zero filter, a four stage semi-Gaussian integrator, and an

amplifier. Emitter followers are used as needed for impedance transformation. The pole zero filter is used to replace the 400 ns integration RC of the preamplifier with a 40 ns RC (for a δ function preamplifier input). Each stage of the semi-Gaussian integrator [18] adds another RC of about 35 ns. A very narrow input signal at the preamplifier has a FWHM of about 170 ns at the PAS output. The purpose of the integration is to reduce the high frequency noise that would otherwise be observed due to the short sampling time of the FADC and to match the memory time of the output waveform to the 10.6 MHz clock speed.

4.3 FADC System

The FADC system performs digitization of analog signals and compaction of the digitized data. The system consists of a) 64 FADC modules (1536 channels total) which digitize analog signals from PAS cards and b) eight compaction modules which read and compact the digitized data from the FADC modules.

4.3.1 FADC Module

A FADC module contains 24 channels in a single width FASTBUS module. The module uses the FASTBUS crate only for DC power and cooling. The analog signals from PAS cards on the detector wall arrive at the FADC modules located in the counting room. The signals are received by a line receiver based on an operational amplifier and fed into an eight bit FADC chip (Sony CXA1016P). The analog baseline is restored by an operational transconductance amplifier (RCA CA3080E) which removes charge accumulated on the final decoupling capacitor. The digitized data from the FADC chip are continuously written into two ECL random access memories

(10422) until a stop signal is issued at the end of the VTPC drift time. A single FADC module dissipates 77W total and can operate at clock speeds up to 35 MHz. For the data described in this paper the FADC module was operated at a 10.6 MHz sampling rate to reduce the total amount of data per event written to magnetic tape.

4.3.2 Compaction Module

A compaction module reads and compacts data from the FADC modules. Each compaction module is a single width FASTBUS slave that communicates with eight FADC modules through a dedicated external bus. After a stop signal, the FADCs are read out and their data are compacted to form groups corresponding to FADC data which are above a programmable threshold and which are contiguous in time. Usually such a group is the result of one chamber pulse. A header word that describes the channel address, time address, and the number of the FADC data points in the group is added to each group. Since the typical signal from the chamber is quite long (1-4 μs), this compaction method minimizes redundant address/time information. The actual FADC values typically make up over 71% of the total formatted data. The remainder is time-channel markers and headers. The average size of pad data for 1.8 TeV events taken with a minimum bias trigger is 11-12 kbytes. The compaction process requires 500 μs per event. The compacted data is stored in local memory, then read via FASTBUS through the SSP.

5 Reconstruction and Systematics

5.1 Wire Reconstruction

A reconstruction program that uses the wire TDC information provides accurate tracking of charged particles throughout the active volume of the VTPC. The reconstruction algorithm has three steps. Track segments are first identified in individual chamber octants. Next, the intercepts of these track segments with the beam axis are used to reconstruct the primary vertex location. Finally, tracks are found and fit across octant and module boundaries. The first two steps are very fast requiring about 300 ms of VAX 8650 CPU time per event. The information from these steps is used for more than just subsequent VTPC reconstruction. The beam collision point is monitored online using the VTPC vertex reconstruction. In addition, the offline calculation of transverse energy corrections in the calorimetry uses this 'fast' vertex location as does the CTC reconstruction. Figure 8 shows the distribution of reconstructed event vertices for a typical run. The third step, track finding across octant and module boundaries, begins by histogramming hits as a function of polar angle with respect to the vertex found in step two. Primary tracks appear as spikes in this histogram. The positions of these spikes determine roads used to associate specific hits to a given track. These associated hits are then fit separately in modules having the same ϕ rotation angle. Finally, three-dimensional information is obtained by combining these fit parameters for tracks crossing module boundaries. All tracks are currently assumed linear. The effect of track curvature due to the axial magnetic field is not observable in wire data for tracks with $P_t > 300$ MeV/c.

This multi-step procedure has the advantage that it uses a single algorithm to

find tracks over the large angular acceptance of the VTPC. As a result, reconstruction efficiency should be smooth as a function of track angle. In addition, this procedure has good efficiency in a high multiplicity environment and is sufficiently fast to allow full reconstruction of a large number of events. The average reconstruction time for events taken with minimum trigger bias is about 1.5 seconds and scales linearly with the number of tracks in the event.

The long drift lengths, ExB forces on drifting electrons, and the wide range of track polar angles seen by the VTPC result in several important systematic effects which require correction. Proper treatment of these effects is important to ensure good tracking efficiency when linking tracks across chamber boundaries. The two largest systematic effects are:

- Variations in drift velocity due to variations in pressure, temperature and gas composition.
- Apparent shifts in track position as a function of the polar production angle.

The chamber is sensitive to small changes in gas conditions which result in variations in drift velocity. This is because the VTPCs operate at a value of E/p of 256 V/cm at one atmosphere, well below that necessary to saturate the drift velocity in Argon-Ethane[19]. At 256 V/cm the variation in drift velocity with E/p is roughly 5×10^{-3} cm/μs (V/cm)$^{-1}$ atm. This corresponds to about 1% change in drift velocity for a change in operating pressure of 25 torr. Variation of as much as 2% in v_d over a period of days is possible. This corresponds to about a 3 mm shift in the apparent position of electrons drifting from near the central grid. Clearly it is important to carefully monitor the drift velocity as a function of time. A technique (described

below) has been developed for doing this directly from the data.

The second major systematic effect is due to the use of leading edge TDC timing to determine track locations in the chamber. The leading electrons contributing to the wire signal arrive from different radial positions within a cell, depending upon the inclination angle of the track relative to the sense wire plane (see Figure 9). For example, the leading electron from a 90° track will arrive from the center of the cell, whereas the leading electron from a 10° track will arrive from the edge of the sense wire cell. This results in an apparent shift in the r position of the wire, or equivalently in the z position of the track. This effect can be quite large for tracks at small polar angles. The corrections for this effect depend on the details of the electric field near the sense wire, diffusion, and ExB forces. These effects have been modeled analytically, but better estimates of these corrections are obtained directly from the data.

Two constraints are useful in determining these corrections. First, tracks crossing the center high voltage grid of the chamber must be continuous. If track segments measured in each half of the same module are not aligned, deviations are assumed to be the result of drift velocity variations and the inclination angle effect mentioned above. The second constraint is that the vast majority of tracks originate from the primary vertex. Using both of these constraints, the drift velocity and the polar angle corrections are extracted from $\bar{p}p$ collision data. This procedure uses a vertex constrained fit which forces track segments to be continuous across the central high voltage grid. The drift velocity, the parameterization of the polar angle correction, the TDC time offset, and the z position of the vertex are fit for each event. Only tracks which are isolated in a single octant and found on both sides of

the high voltage grid in a single module are used in the fit. Each measured time t_i on a track corresponds to a location z_i parameterized as:

$$z_i = z_s \pm (v_d(t_i - t_o) + f(\theta)) \tag{1}$$

where

z_s is the position of the sense wire plane for that particular hit

v_d is the drift velocity

t_i is the leading edge time from wire i

t_o is a global time offset related to the difference between the actual interaction time and the TDC stop time.

$f(\theta)$ is the polar angle correction

The "+" in eq. 1 corresponds to tracks drifting towards smaller values of z, while "−" refers to tracks drifting in the opposite direction. An event χ^2 is formed by forcing the vertex z position to be the intercept for all the tracks. By minimizing this χ^2 with respect to the event vertex, v_d, t_o and the parameters for $f(\theta)$, one can derive these constants on an event-by-event basis. Figure 10 shows the wire hits and the track fits used to determine these constants for a typical event.

The results of these fits yield a measurement of drift velocity for each event. When averaged over only a few events, a value accurate to $< 0.5\%$ can be obtained. For the majority of runs, the drift velocity is found to be about 4.2 cm/μs. The polar angle correction is approximated by quadratic splines for dip angles between 30° and 120°, and is assumed linear for lower angles. The asymptotic form of this

correction has a slope which is equal to half the cell spacing. This agrees with expectations based upon purely geometric grounds since for small polar angles the earliest arriving electrons are those drifting from near the edge of the sense wire cell. Figure 11 shows a scatterplot of the track mismatch (Δz) as a function of $\cot(\theta)$.

5.2 Pad Reconstruction

The VTPC ϕ reconstruction uses pad data and the r-z wire reconstruction information to obtain complete three-dimensional tracks. The raw FADC data is converted into calibrated ADC data by subtracting pedestals and applying electronic gain corrections. The induced charge distribution on a pad row is processed for each FADC time slice. The ϕ position is determined by fitting a Gaussian to the measured charge distribution. The z is determined from the time address. An approximate r is determined by the pad row. If this distribution has more than one peak, they are separated by an iterative process which subtracts contamination from adjacent peaks. At present, the minimum resolvable ϕ is about one pad spacing (1.4 cm).

The resulting points for each pad row form a group in the z-ϕ plane. Groups associated with tracks from the primary vertex are easily recognizable straight lines in the z-ϕ plane. These lines have small slopes for $P_t > 300$ MeV/c and are usually well separated in one of the three measured coordinates. This procedure for pattern recognition is insensitive to errors in ϕ ($\sim 3°$) and z ($\sim$2 cm). The lines are then matched with tracks found in the r-z wire reconstruction and the points associated with the lines are fit in the z-ϕ plane. This fit combined with the r-z information yields complete three dimensional tracks.

5.3 dE/dx

The FADC system is also used to measure the dE/dx of charged particles. The reconstructed r-z track information is used to generate a z window for each wire FADC channel. The FADC samples within these windows are collected for each track. After pedestal subtraction, gain corrections, and discarding the largest 35% of the samples, the mean value of ionization per unit track length is computed.

6 Performance

Figure 12a and 12b show displays of typical 1.8 TeV collisions observed with the VTPC system. Figure 12a show a typical event taken with a high E_t threshold calorimetry trigger. Figure 12b shows an event in the VTPC with two $\bar{p}p$ interactions in the same crossing.

Several factors contribute to the observed wire resolution. These factors depend upon the angle and position of the track in the chamber. For tracks near 90° (i.e., parallel to the sense wire plane) longitudinal diffusion of electrons dominates the measured resolution. For tracks highly inclined with respect to the wire plane, different effects dominate at different drift distances. Ionization fluctuations dominate the resolution for short drift distances and transverse diffusion dominates for long drift distances. Figure 13 indicates the z resolution as a function of polar angle θ averaged over the drift length. For 90° tracks the resolution is 420 μm, rising to 1100 μm at 11°. These data were taken at a luminosity of $2 \times 10^{27}\text{cm}^{-2}\text{s}^{-1}$. Figure 14 shows the z resolution squared as a function of drift distance for 90° tracks. This plot is expected to be approximately linear because longitudinal diffusion fluctuations scale

as the square root of the drift distance. The line superimposed on the plot represents the best fit to the data. The position resolution near the sense wires is about 200 μm, while the resolution for the longest drift times is about 550 μm.

The impact parameter b of tracks with the primary vertex is defined by the following:

$$b = (z - z_{vertex}) \cdot \sin(\theta)$$

Figure 15 shows a histogram of impact parameters of reconstructed wire tracks for a sample of events taken with a minimum trigger bias. The RMS of the distribution is about 0.3 cm.

Multiple track separation in z is determined primarily by the pulse width of signals from a single track. At 90°, the pulse width for a track corresponds to about 0.5 cm of drift length. The effective pulse width grows as $\cot(\theta) \cdot W_s$ (where W_s is the wire spacing) for smaller angle tracks.

The chamber precision in ϕ is studied using the residuals from the pad data. For a given FADC sampling, the ϕ residual from the fit line in the z-ϕ plane is calculated for isolated tracks. The ϕ residual is converted into an r-ϕ residual using the r information of the track. Figure 16 shows the r-ϕ residual distribution, which is fit to a Gaussian with a σ of 418 μm. The residual σ is about 350 μm per sampling for a very short drift length (~1-2 cm) and 400-450 μm per sampling for a larger drift length. There are 40 FADC measurements made on a track that extends across the full 15.25 cm drift region. Because of correlations in successive FADC samplings, the number of independent measurements is typically about 15. The overall chamber precision is therefore of order 100 μm.

Over the course of the four month 1987 run, the VTPC modules were operated

at nominal voltages for $\bar{p}p$ integrated luminosity of 70 nb^{-1} as well as many days of stored proton beam. No evidence was observed for aging effects.

7 Space Charge

One of the limiting factors in the VTPC at high luminosity is expected to be buildup of positive ions in the drift region causing distortions in the drift fields. For our drift field, the positive ion drift velocity is so low that tens of milliseconds are required to traverse the drift region. The maximum ion current density that the drift region can support is estimated in MKS units to be:

$$J_{max} = (1.5)^2 E_d^2 \frac{\mu \epsilon_o}{2d}$$

where E_d is the electric field strength, μ is the positive ion mobility, ϵ_o is the permittivity of free space, and d is the length of the region. For ion current densities that are 10% of the maximum, the space charge causes equipotential displacements in the drift direction of about 2 mm. This should cause distortions in the track reconstruction of the same order of magnitude. It is expected that this current density will be reached at luminosities of order $0.5 \times 10^{30} cm^{-2} s^{-1}$ for our current chamber operating conditions. At the end of the 1987 CDF run, luminosities of $\sim 1 \times 10^{29} cm^{-2} s^{-1}$ were reached.

The effect of drift field distortions is studied by examining systematic shifts of track residuals as a function of luminosity. Tracks which have at least 15 hits in a single octant are selected for this study. A straight line fit of these tracks is made using hits only on the middle 15 wires of the chamber. The results of these fits are extrapolated to both the innermost and outermost wires hit in the chamber. Any

drift field distortion appears as a systematic shift of the residuals of the inner and outer wires away from zero. At low luminosity, $\sim 1 \times 10^{27}\mathrm{cm}^{-2}\mathrm{s}^{-1}$ the measured shifts are consistent with zero. At luminosities $\sim 1 \times 10^{29}\mathrm{cm}^{-2}\mathrm{s}^{-1}$, distortions as large as 800 μm are observed. The distortion is largest at the innermost wires and substantially smaller, < 300 μm, for the outermost wires. This variation of distortion with radius is to be expected because the ion density should be larger closer to the beam axis. Since the Tevatron operating conditions are usually quite stable over the period of a typical data run, it is expected that the data can be corrected for these effects.

For future higher luminosity running, the situation can be improved by raising the electric field and/or shortening the drift distance d_{drift}. Tracking distortions from positive ion effects should scale roughly as $1/d^3_{drift}$. One power of the drift distance is due to the increased number of positive ions produced at a given luminosity for a larger active chamber volume. Another power of the drift distance is due to the magnification of the distortions by a longer lever arm. The third power of drift distance results from the longer time that the positive ions spend in the drift region. Shorter versions of the present chambers with higher drift fields are being considered for the future. Reasonable performance with luminosities of $10^{31}\mathrm{cm}^{-2}\mathrm{s}^{-1}$ should be attainable.

8 Acknowledgements

The authors wish to thank all members of the CDF collaboration for their help and advice throughout the course of the project. The success of this system was the result

of the hard work of many individuals. However, the authors wish to especially thank A. Tollestrup, E. Erdos, W. Foster, S. Gonzalez, A. King, M. Kurisu, R. Paoletti, A. Para, D. Tousignant, R. Wagner, and J. Welch for their special efforts on this project. The authors also wish to thank V. Radeka of B.N.L. for his help in the early stages of the preamplifier design.

References

[1] F. Abe *et al* ., The Collider Detector at Fermilab, submitted to NIM.

[2] F. Bedeschi *et al* ., Design and Construction of the CDF Central Tracking Chamber, submitted to NIM.

[3] M. Atac *et al* ., Radial wire Drift Chambers for CDF Forward Tracking, submitted to NIM.

[4] Rohacell foam is a rigid acrylic foam (density = 0.05) distributed by Cyro Industries, 25 Executive Blvd, P.O. Box 579, Orange, CT. 06477 Tel. (201)930-0100.

[5] Kapton is a trademark for a polyimide film manufactured by DuPont de Nemours, E.I., Co., Wilmington, Del. 19898.

[6] Great Lakes Carbon Co., P.O. Box 810, Rockwood, Tenn. 37854 Tel. (615)354-4120.

[7] Gantois, B.P. 307-88105 St.Die Cedex, France. Tel (29)552143.

[8] Polygon Co., P.O. Box 176, Walkerton, IN 46574 Tel (219)586-3122.

[9] Methode Development, 7447 W. Wilson, Chicago, IL 60656. Tel (312)867-9600.

[10] Sheffield Measurement Division, Warner-Swasey/Acoss and Trecker Co., P.O. Box 1127, Dayton, OH 45401-1127.

[11] Junkosha Co., Ltd., Hanno Plant, 3-1 Ashikariba, Hanno-shi, Saitama-ken 357 Japan, Tel: 04297-3-2261, Telex: 2954185 JUN HP.

[12] T.& B./Ansley, 4371 Valley Blvd., Los Angelos, CA 90032.

[13] Hitachi Cable Ltd., Electronic Wire & Cable Design Dep., Hitaka Works, 5-1-1 Hitaka-cho, Hitachi-shi, Ibaraki-ken 319-14 Japan.

[14] Fujitsu Microelectronics Ltd., Solid State Department, 18-Mori Building, 2-3-13 Toranomon, Minato-ku, Tokyo, Japan.

[15] R. J. Yarema *et al* . A Surface Mount Amplifier-Shaper-Discriminator and Preamplifier for the Fermilab CDF Tracking Chambers, IEEE Trans. NS-33(1986)933.

[16] LeCroy Research Systems Corp., 700 S. Main Street, Spring Valley, New York 10977.

[17] H. Brafman *et al* ., IEEE Trans. NS-32(1985)336.

[18] R. A. Boie *et al* ., IEEE Trans. NS-28(1981)603.

[19] Ma. *et al* MIT Technical reports 129 and 130 (1982).

Table 1: VTPC Specifications

Dimensions:	# modules	8
	Module length	35.3 cm
	Modules spacing	35.94 cm
	Max. active radius:	21 cm
	Min. active radius:	7 cm
	Drift Length:	15.25 cm
End Caps:	Sense Wires:	24 /octant
		6.336 mm spacing
		15 μm gold-plated tungsten.
	Field Wires:	24 /octant
		63 μm Copper/Beryllium
	Cathode Pads:	24 pads/octant, in 3 rows
		4.12 cm in r by $\approx$ 1.4 cm in r-ϕ
	Resistive ink:	10 MΩ/square
Field Cage:	Material:	Kapton/Rohacell foam laminate
		epoxy/graphite-foam support frame
	Electrodes	3.175 mm overlapping strips on 2.38 mm centers
	Central grid	ss screen 50 μm wires on 1000 μm centers
	Cathode grid	ss screen 50 μm wires on 500 μm centers
Magnetic Field:	B_{axial}	1.5 Tesla
	$B_{radial}(max)$	$< 1\% B_{axial}$
Drift Field:	E_{drift}	256 V/cm
Gas :	Argon-Ethane	50/50 at 1 atm.
	Drift velocity	42 μm/ns
Voltages:	Cathode	-2.5 kV
	Field Shaping	-1.6 kV
	Central grid	-6.4 kV
	Sense wire	Ground
Electronics:	# Wire channels	3072
	# Pad channels	768
	# dE/dx channels	768

Figure Captions

- Figure 1. Cross section through 1/4 of the CDF central detector showing the location of the VTPC system. Drift spaces marked with an * are instrumented for pad and dE/dx readout with FADCs.
- Figure 2. An isometric view of two VTPC modules. They are rotated in ϕ by 11.3° with respect to each other.
- Figure 3. Construction details of the VTPC proportional chamber region.
- Figure 4. Four VTPC modules in their service position during installation. The preamplifier cards and ribbon coax cables are in place on the modules. The CTC endplate is seen in the background.
- Figure 5. Material traversed versus polar angle.The dotted line indicates material traversed before entering the active volume of the VTPC. The dot-dash line indicates the total amount of material crossed by a particle as it exits the VTPC system. The solid line and arrows indicate the average total material traversed before entering the active volume of the CTC or FTC.
- Figure 6. Simplified schematic of VTPC wire electronics.
- Figure 7. Simplified schematic of VTPC pad electronics.
- Figure 8. Distribution of event vertices along the beam axis for a typical CDF run.
- Figure 9. Leading electron effect due to track polar angle θ. The first electrons arriving at the sense wire come from different radial regions in the cell and follow different drift trajcetories, depending on track polar angle θ.

- Figure 10. The r-z projection of a typical event used in determining the VTPC reconstruction constants. Shown are the track fits constrained to a common vertex, and the wire hits used in these fits.

- Figure 11. Scatterplot of the mismatch in z for tracks crossing the center grid as a function of cotan(θ).

- Figure 12. Event displays showing an r-z projection of the VTPC wire hits. a) A typical large E_t triggered event. b) Two 1.8 TeV $\bar{p}p$ collisions occuring in the same Tevatron bunch crossing. Note that the vertical scale in these displays is magnified by a factor of four relative to the horizontal scale.

- Figure 13. z resolution per wire averaged over drift distance as a function of track angle θ.

- Figure 14. z resolution squared per wire for 90° tracks as a function of drift distance.

- Figure 15. Distribution of impact parameters for all tracks. The sigma of the distribution is 0.3 cm.

- Figure 16. Distribution of r-ϕ residuals from pad data. An r-ϕ residual is calculated for isolated tracks for each FADC sampling. The σ of the distribution is 418 μm.

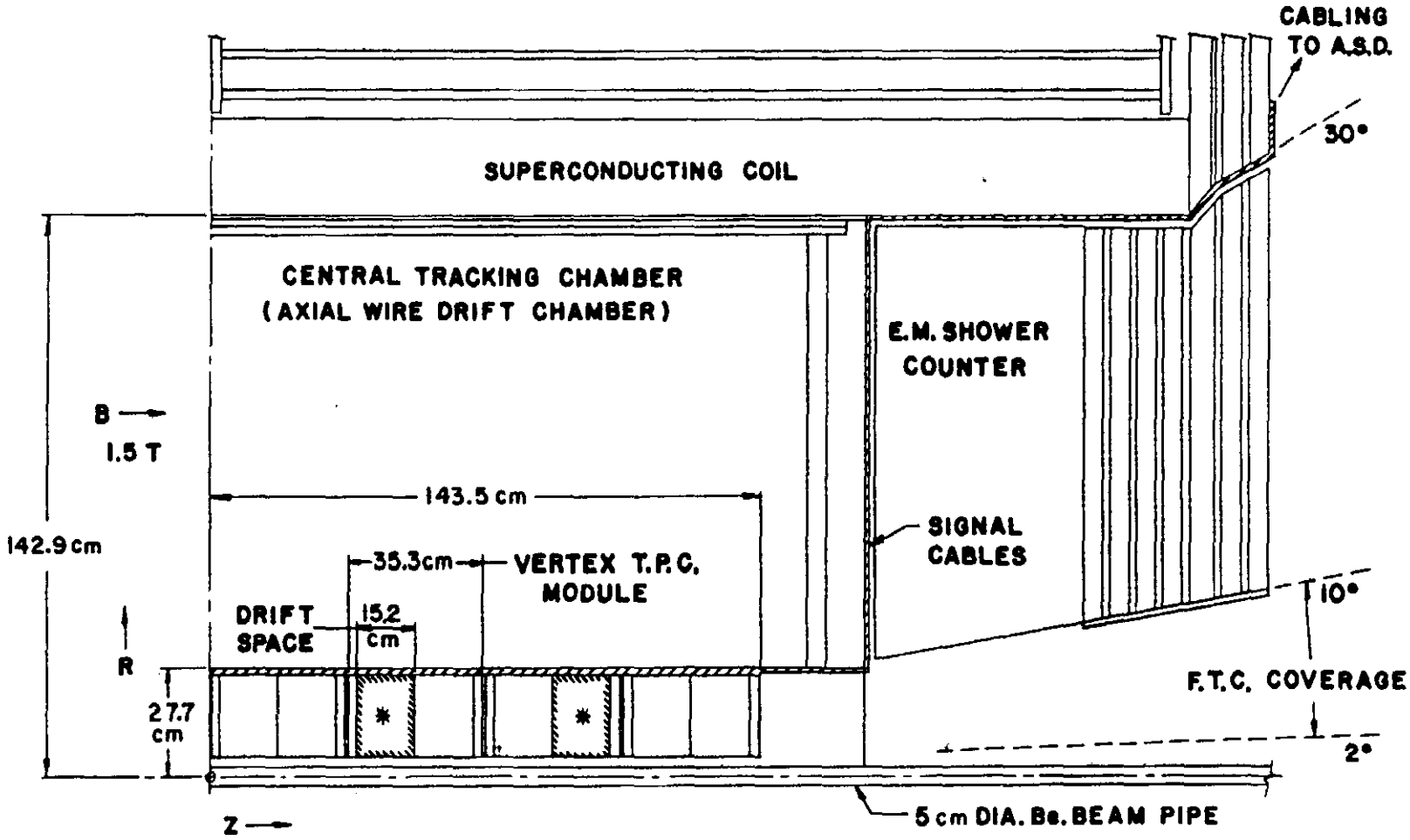
CABLING
TO A.S.D.
30°
SUPERCONDUCTING COIL
CENTRAL TRACKING CHAMBER
(AXIAL WIRE DRIFT CHAMBER)
E.M. SHOWER
COUNTER
B
1.5 T
143.5 cm
142.9 cm
35.3cm
VERTEX T.P.C.
MODULE
SIGNAL
CABLES
10°
DRIFT
SPACE
15.2
cm
R
27.7
cm
F.T.C. COVERAGE
2°
5 cm DIA. Be. BEAM PIPE
Z

Fig 1

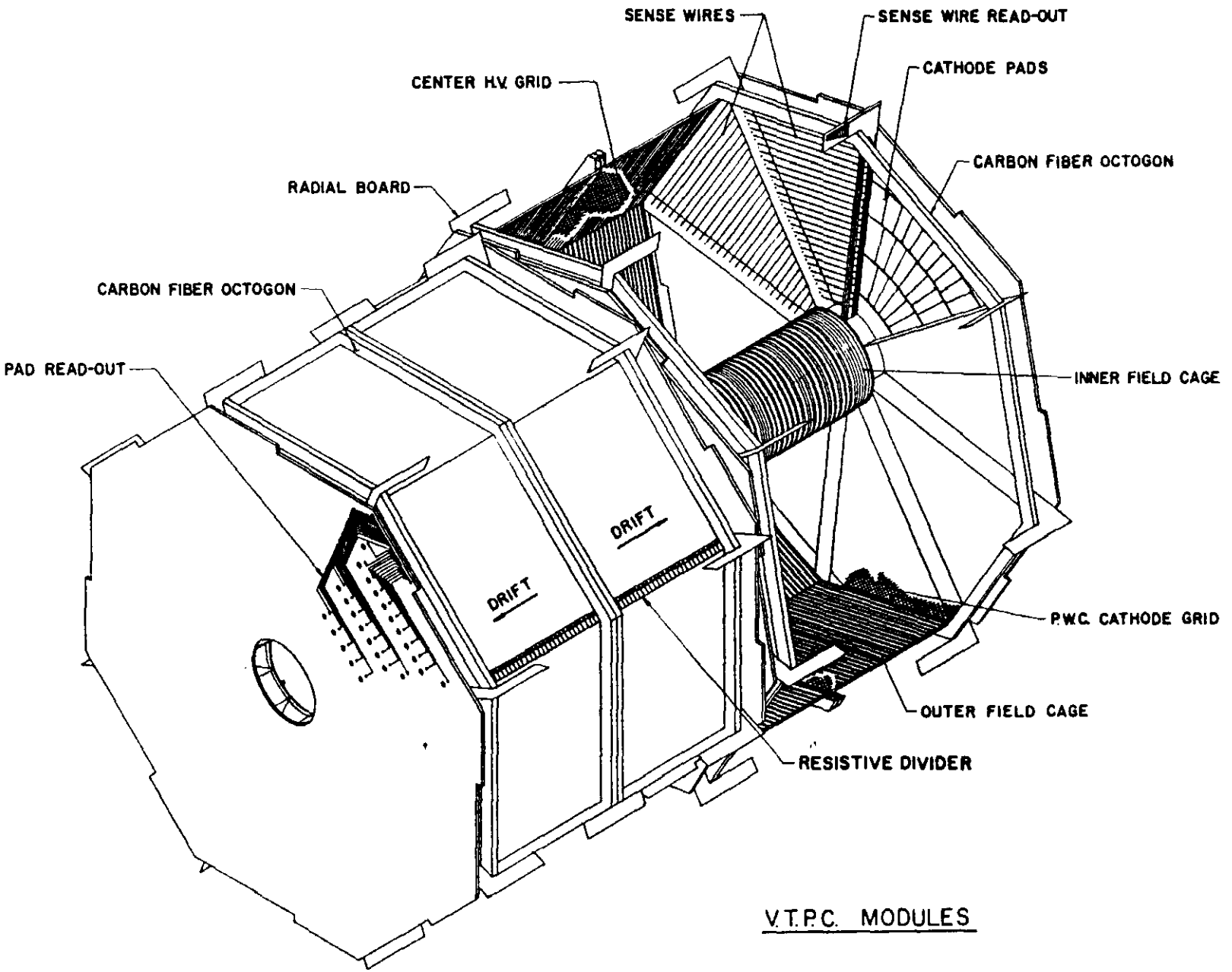

V.T.P.C. MODULES

Fig 2

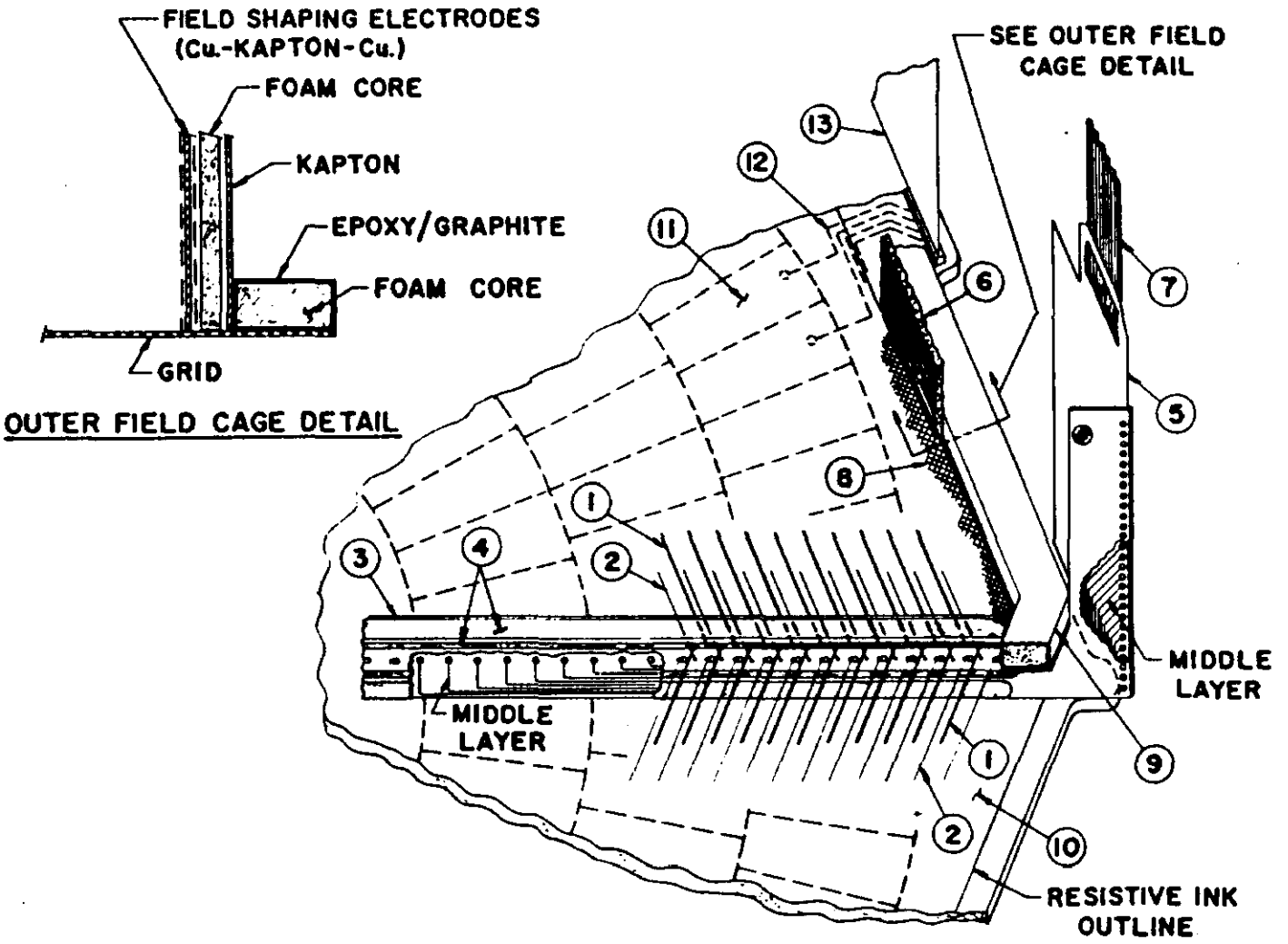

1- FIELD SHAPING WIRE
2- SENSE WIRE
3- MULTI (3) LAYERED RADIAL BOARD
4- FIELD SHAPING ELECTRODES
5- WIRE PRE-AMP.
6- OUTER FIELD CAGE
7- MINI.-COAX. CABLE (25)
8- CATHODE GRID
9- EPOXY/GRAPHITE-FOAM FRAME
10- RESISTIVE INK CATHODE
11- CATHODE PAD
12- PAD READ-OUT
13- PAD PRE-AMP.

Fig 3

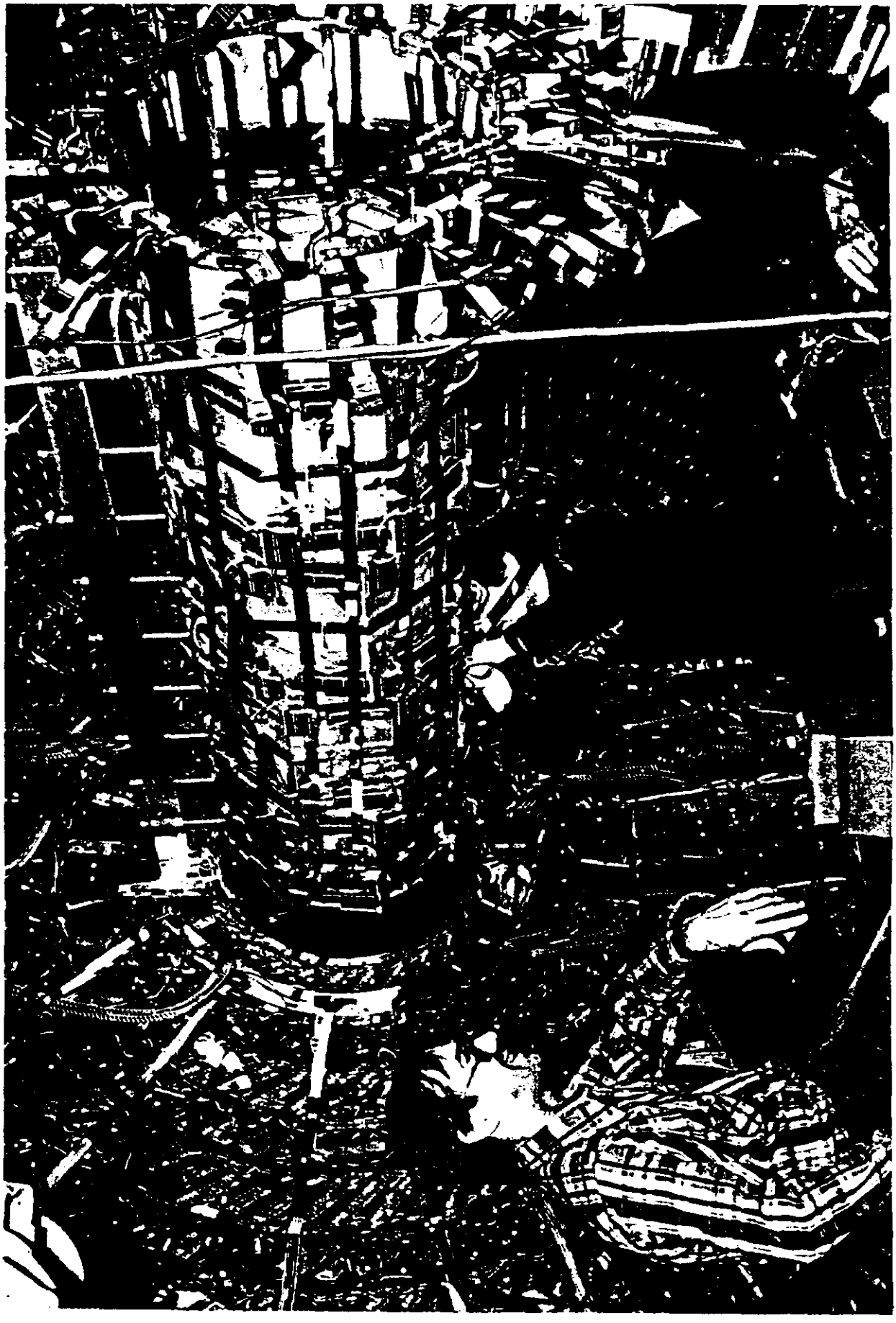

Fig 4

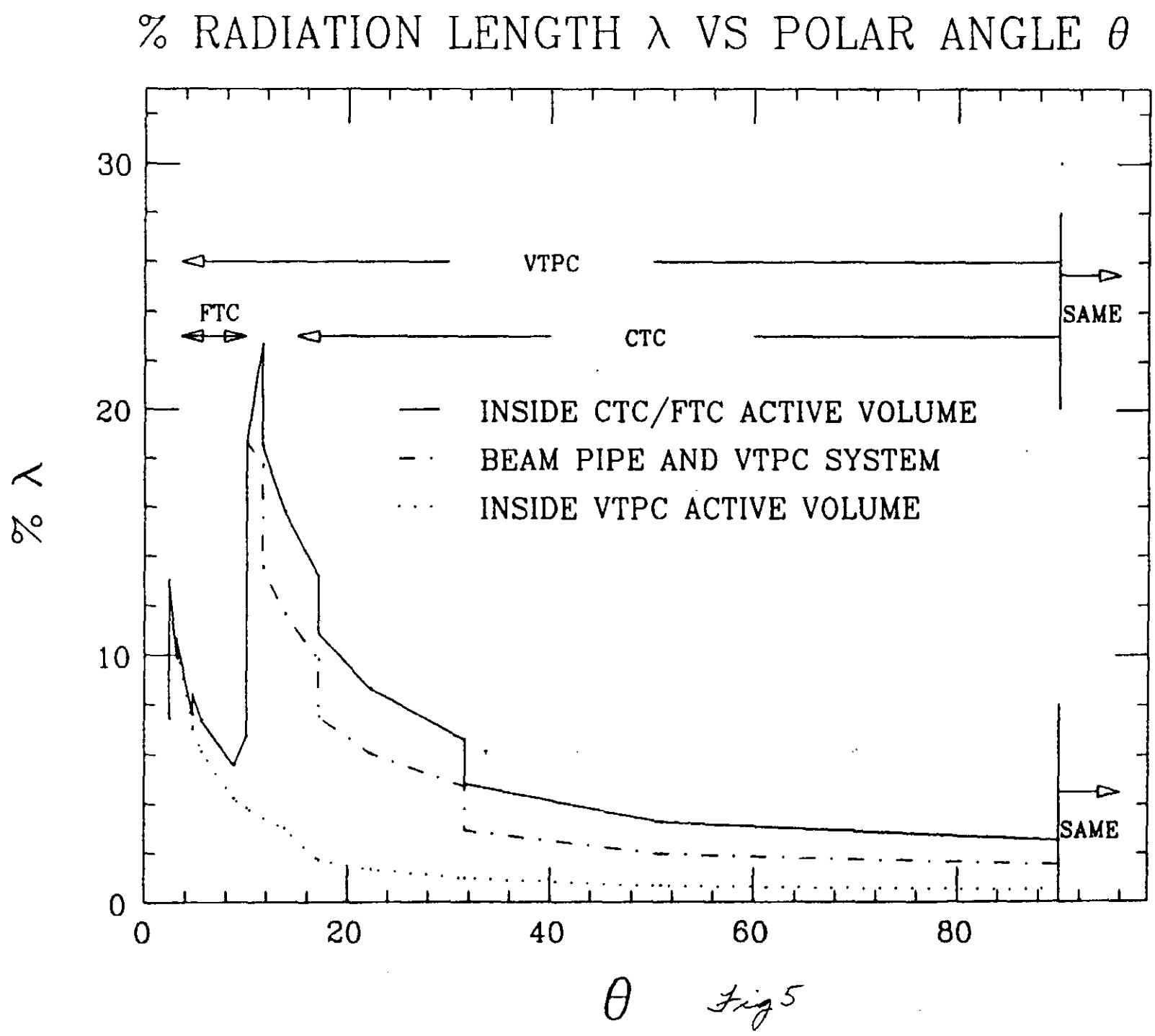
% RADIATION LENGTH λ VS POLAR ANGLE θ
30
20
10
0
% λ
VTPC
FTC
CTC
SAME
SAME
INSIDE CTC/FTC ACTIVE VOLUME
BEAM PIPE AND VTPC SYSTEM
INSIDE VTPC ACTIVE VOLUME
0
20
40
60
80
θ

Fig 5

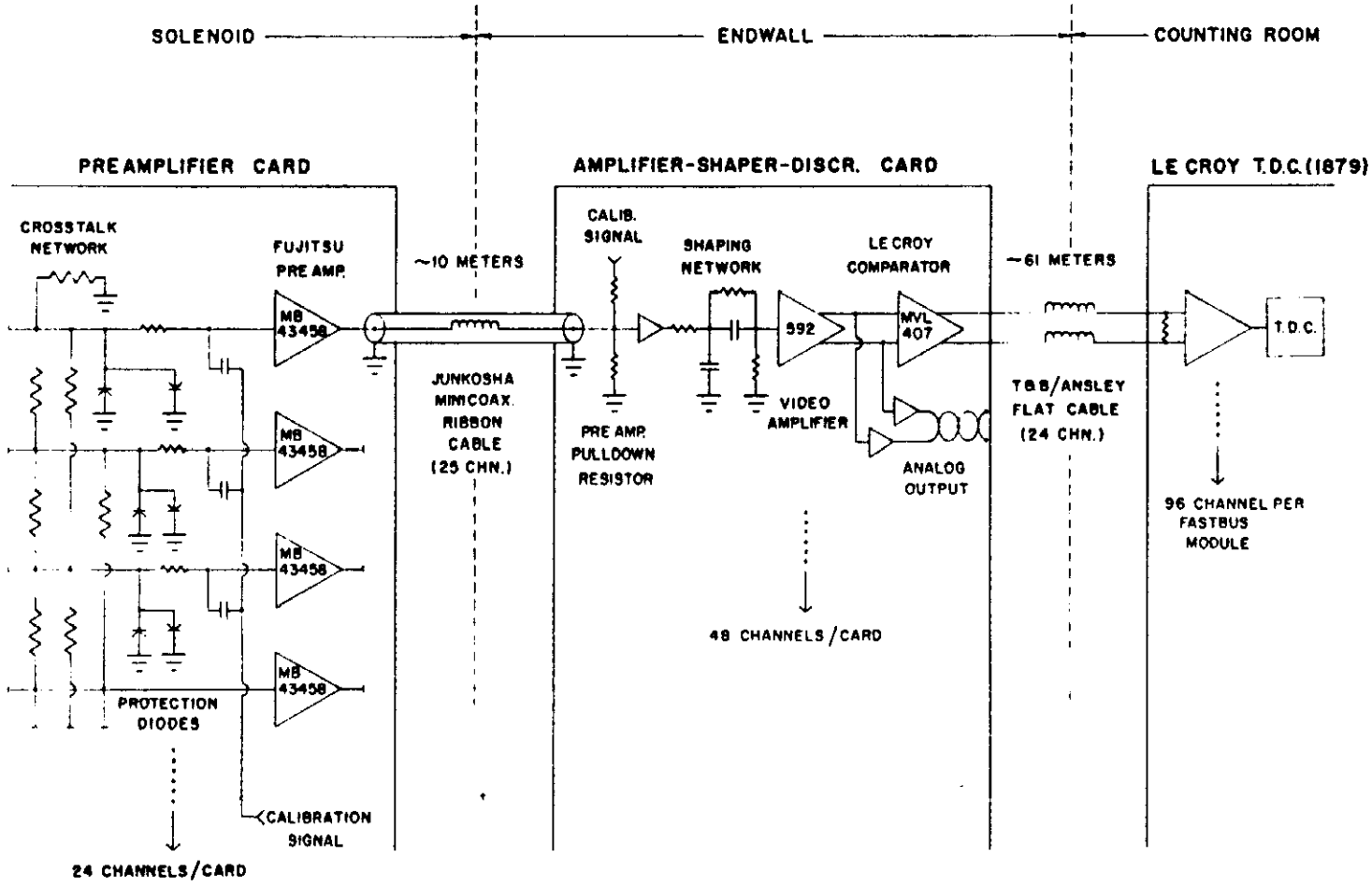
SOLENOID
ENDWALL
COUNTING ROOM
PREAMPLIFIER CARD
AMPLIFIER-SHAPER-DISCR. CARD
LE CROY T.D.C.(1879)
CROSSTALK NETWORK
FUJITSU PRE AMP.
MB 43458
~10 METERS
JUNKOSHA MINICOAX. RIBBON CABLE (25 CHN.)
CALIB. SIGNAL
PRE AMP. PULLDOWN RESISTOR
SHAPING NETWORK
592
LE CROY COMPARATOR
MVL 407
VIDEO AMPLIFIER
ANALOG OUTPUT
~61 METERS
T&B/ANSLEY FLAT CABLE (24 CHN.)
T.D.C.
96 CHANNEL PER FASTBUS MODULE
48 CHANNELS/CARD
PROTECTION DIODES
CALIBRATION SIGNAL
24 CHANNELS/CARD

Fig 6

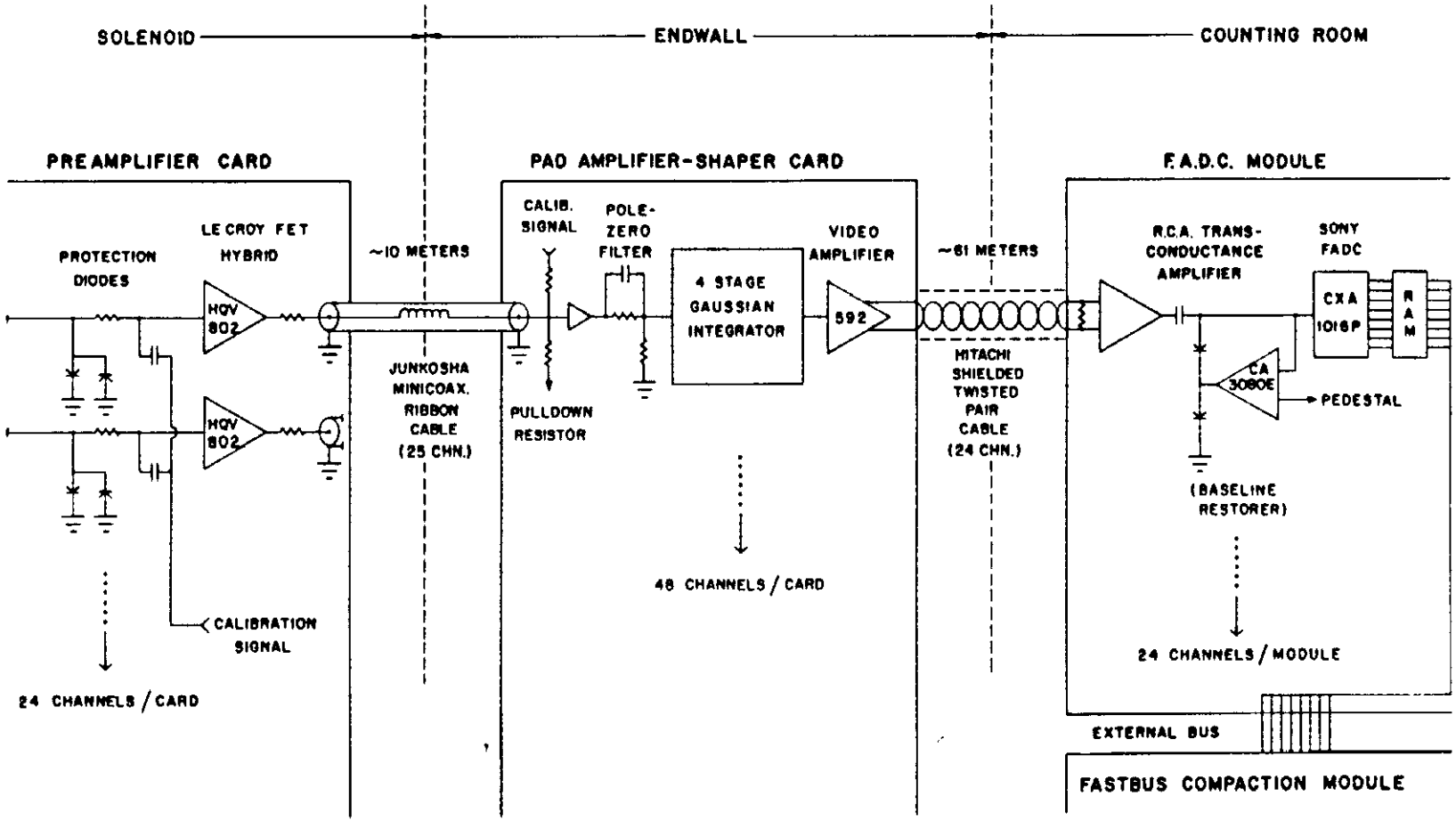
SOLENOID
ENDWALL
COUNTING ROOM
PREAMPLIFIER CARD
PAD AMPLIFIER-SHAPER CARD
F.A.D.C. MODULE
PROTECTION DIODES
LE CROY FET HYBRID
HQV 802
HQV 802
~10 METERS
JUNKOSHA MINICOAX. RIBBON CABLE (25 CHN.)
CALIB. SIGNAL
POLE-ZERO FILTER
PULLDOWN RESISTOR
4 STAGE GAUSSIAN INTEGRATOR
VIDEO AMPLIFIER
592
48 CHANNELS / CARD
~61 METERS
MITACHI SHIELDED TWISTED PAIR CABLE (24 CHN.)
R.C.A. TRANS-CONDUCTANCE AMPLIFIER
SONY FADC
CXA 1018P
RAM
CA 3080E
PEDESTAL
(BASELINE RESTORER)
24 CHANNELS / MODULE
CALIBRATION SIGNAL
24 CHANNELS / CARD
EXTERNAL BUS
FASTBUS COMPACTION MODULE

Fig 7

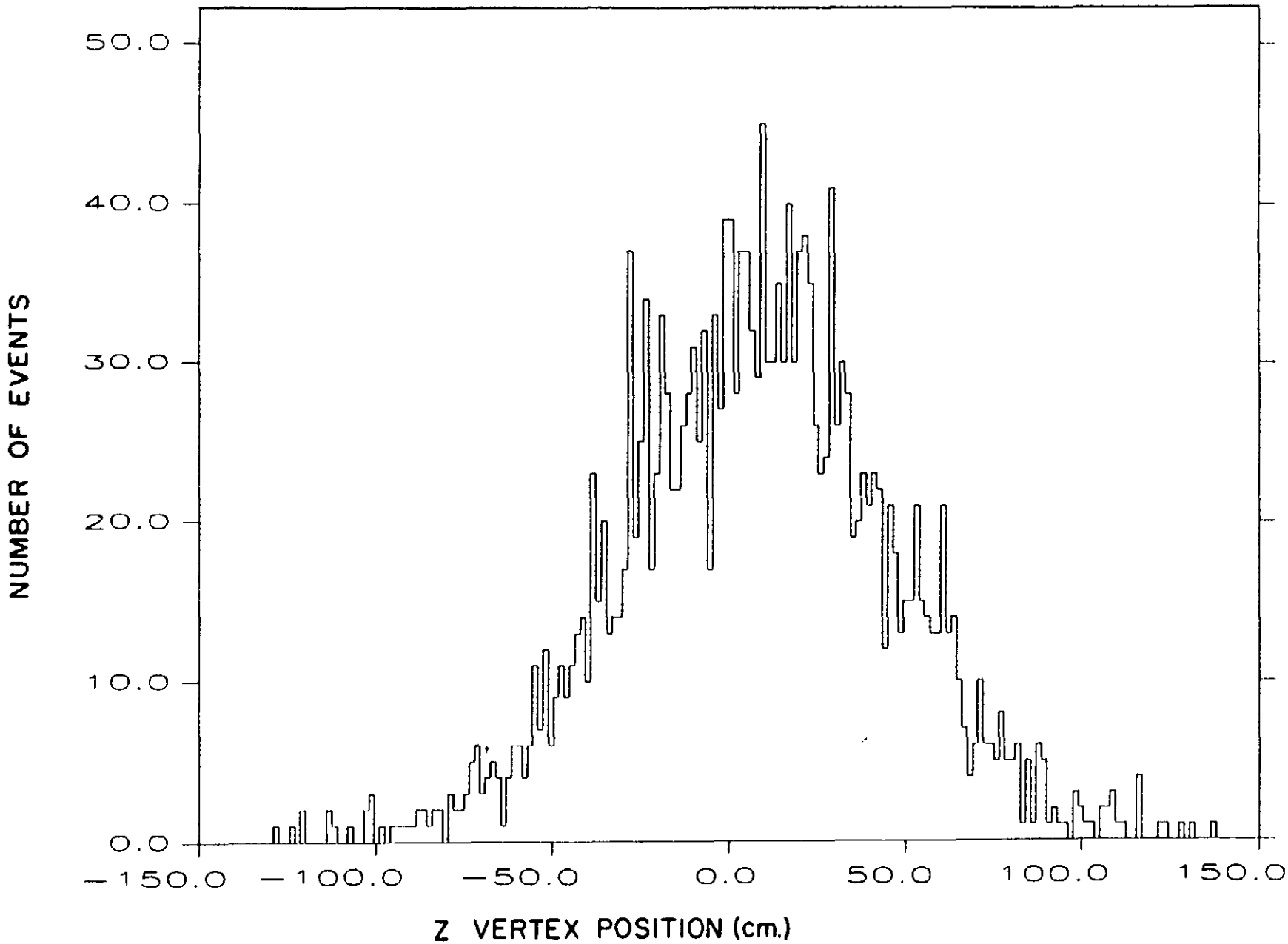
50.0
40.0
30.0
20.0
10.0
0.0
NUMBER OF EVENTS
−150.0
−100.0
−50.0
0.0
50.0
100.0
150.0
Z VERTEX POSITION (cm.)

Fig 8

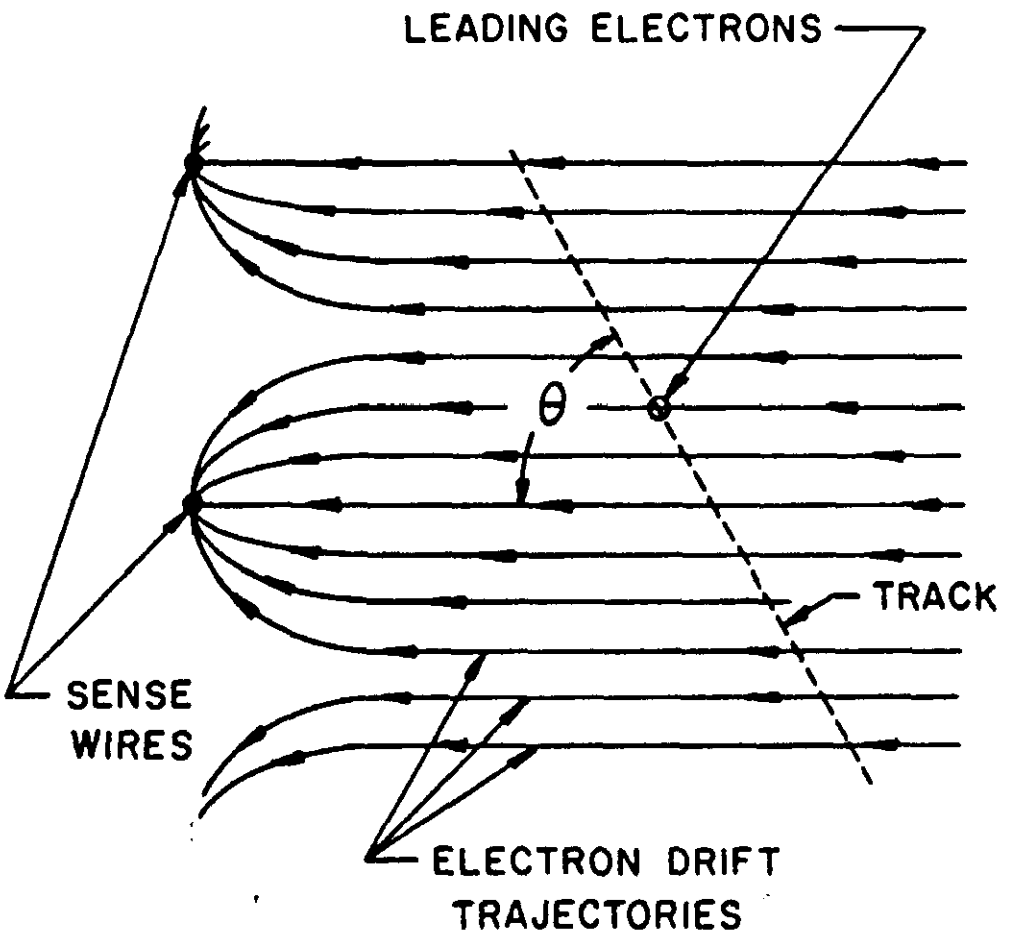
LEADING ELECTRONS
θ
TRACK
SENSE
WIRES
ELECTRON DRIFT
TRAJECTORIES

Fig 9

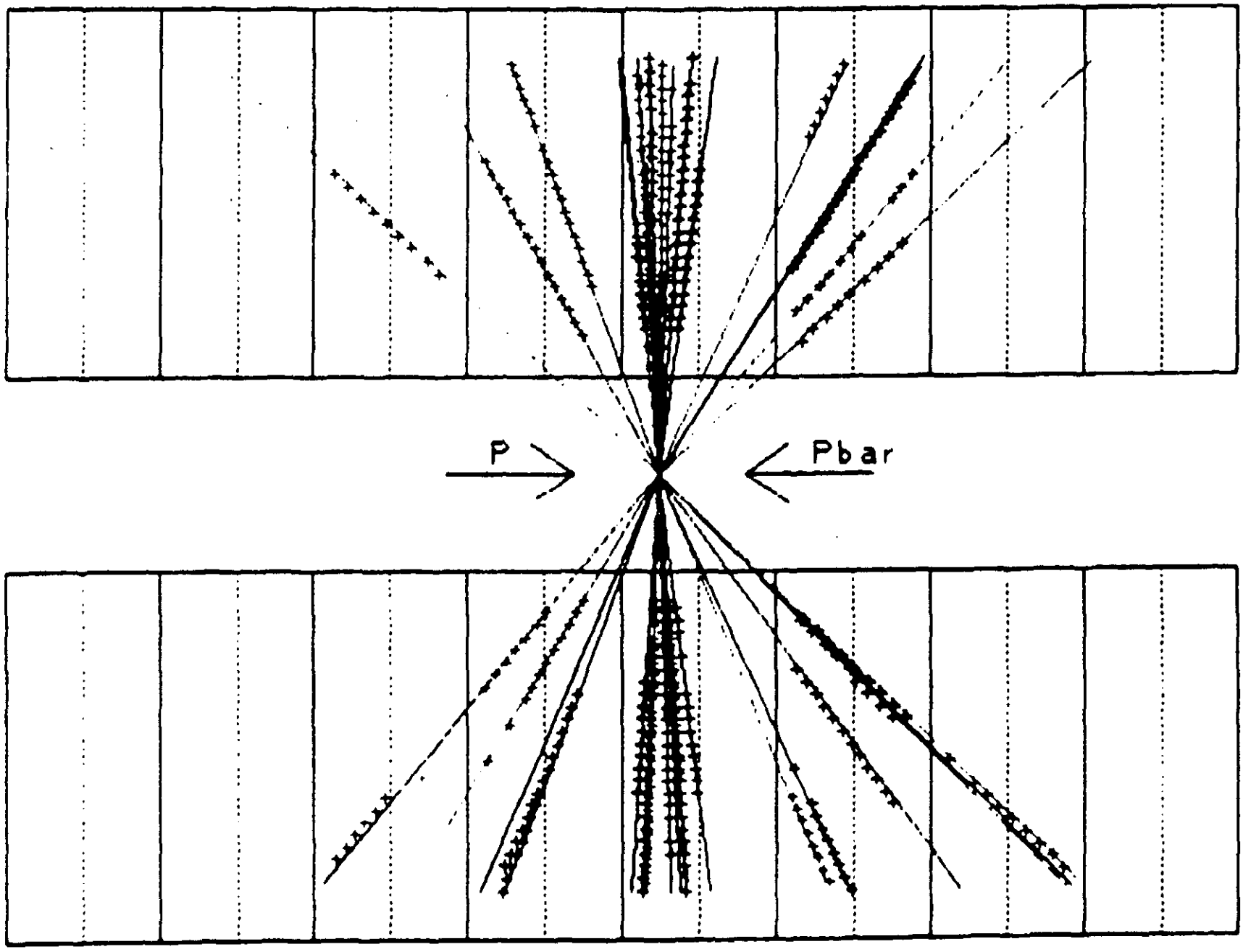

Fig 10

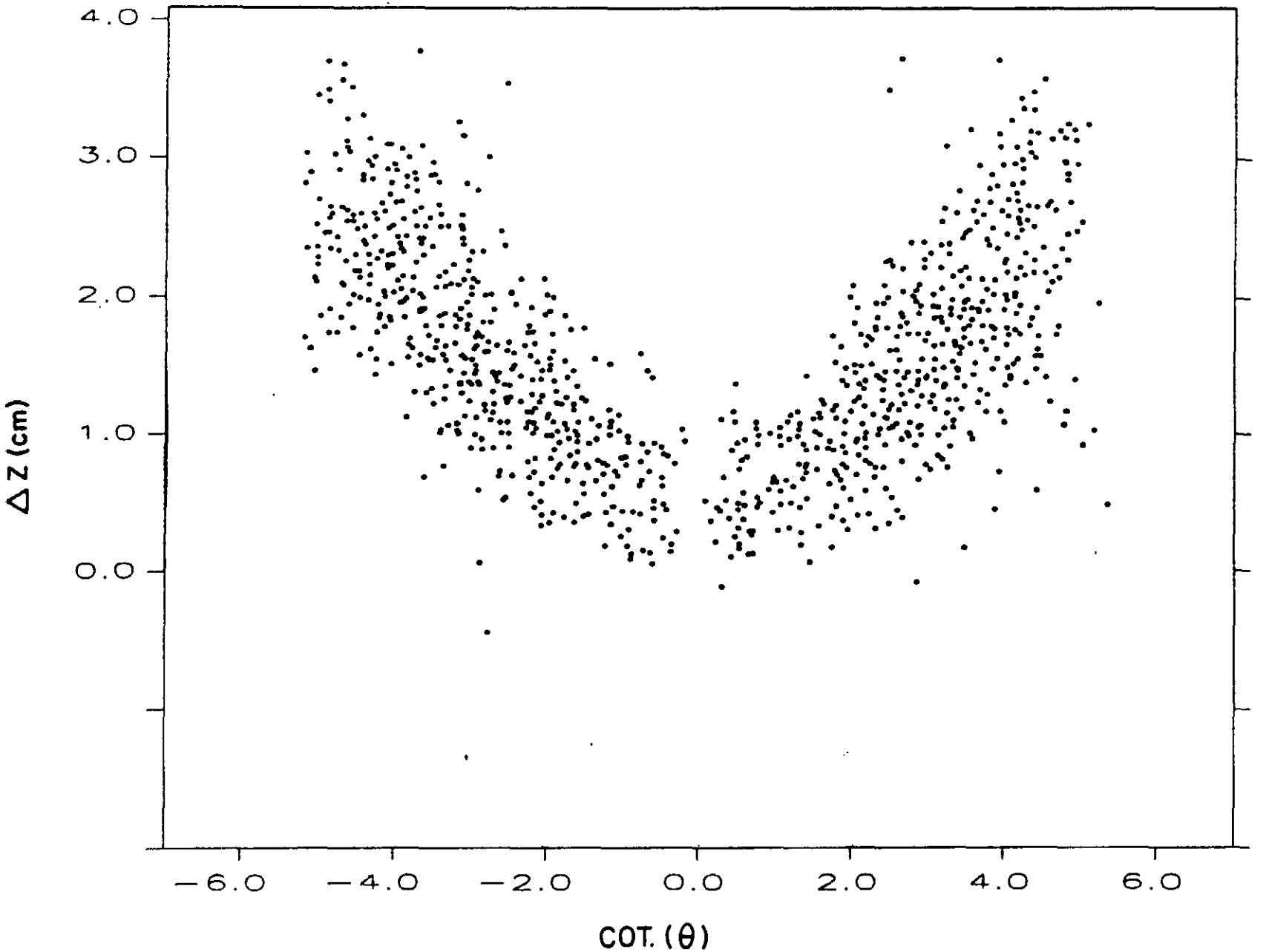

Fig 11

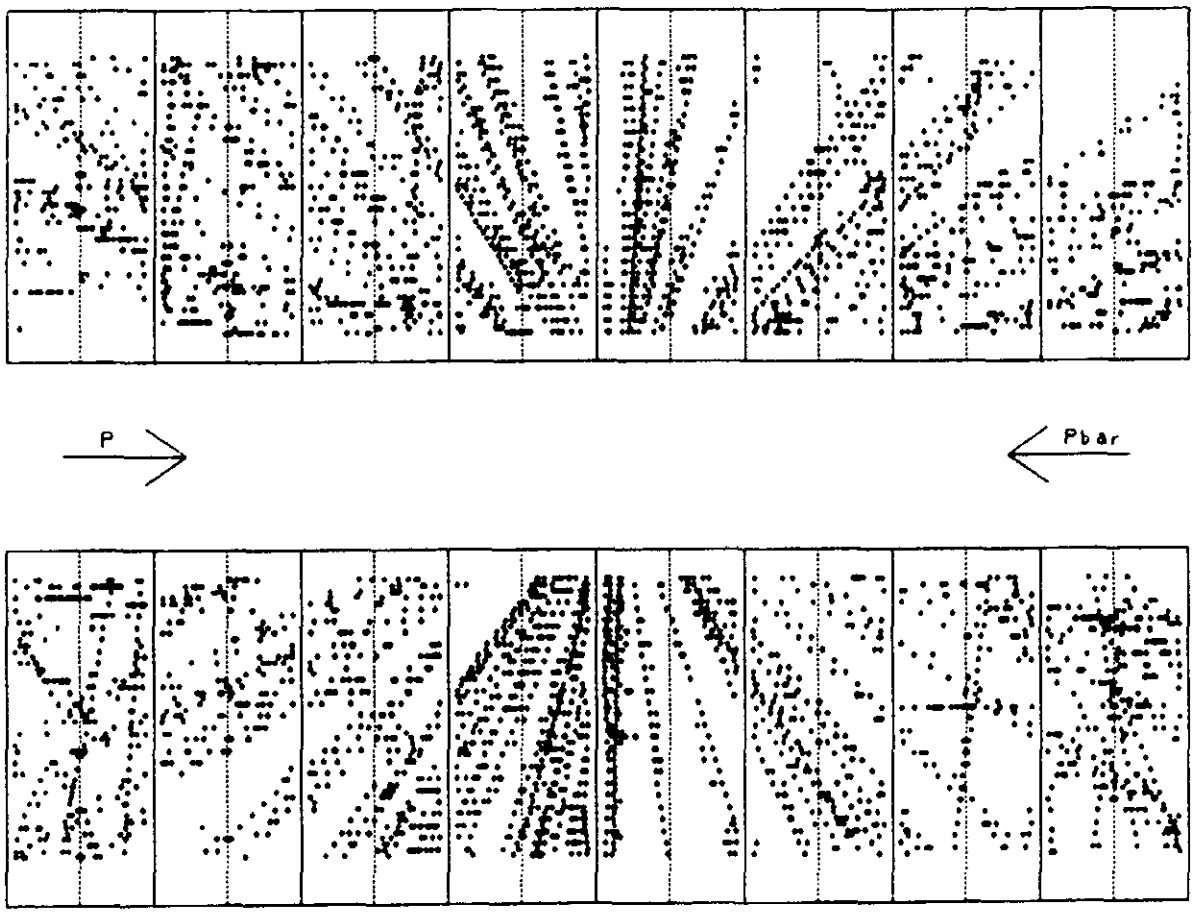

Fig 12a

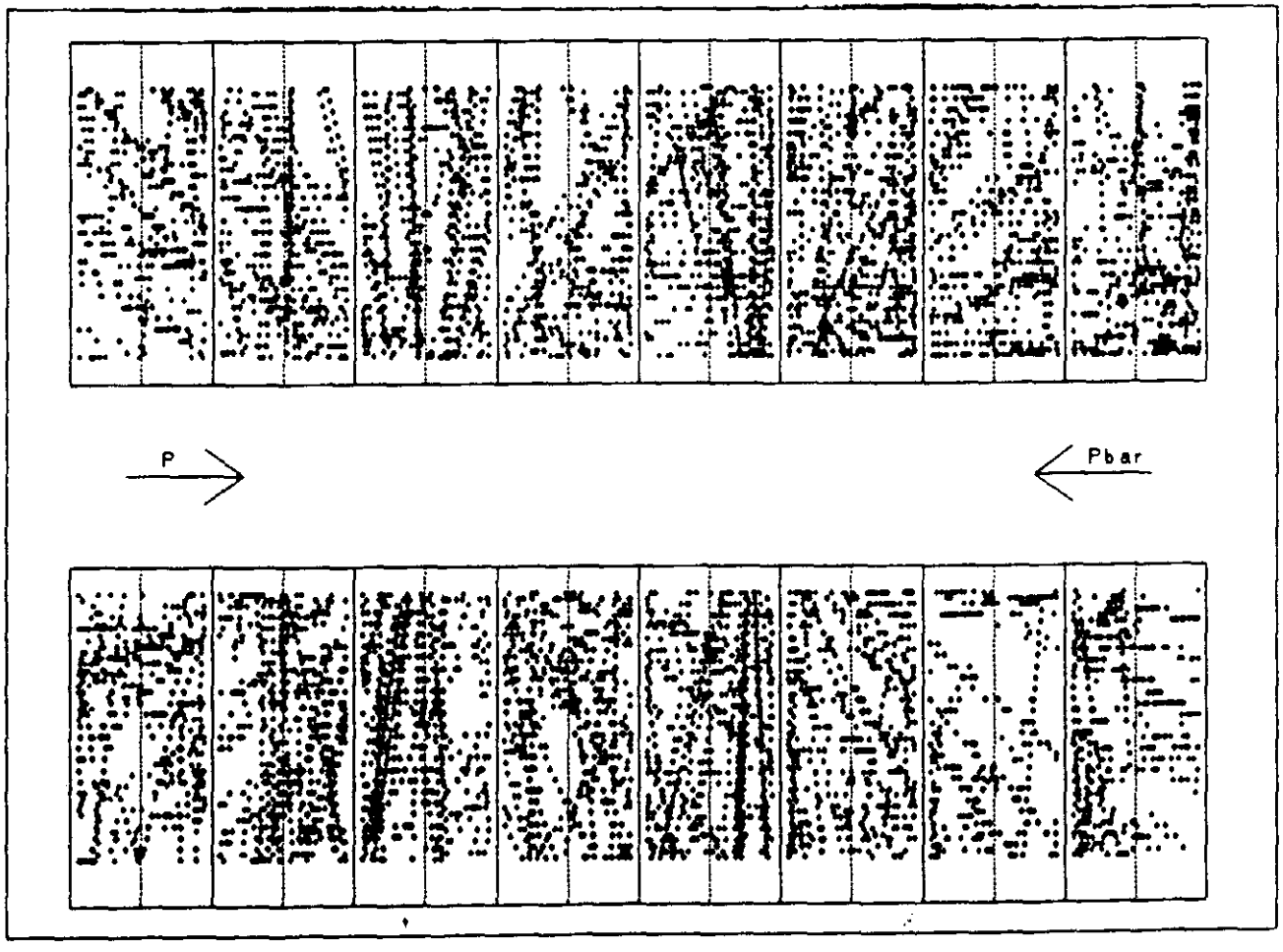

Fig 12 (b)

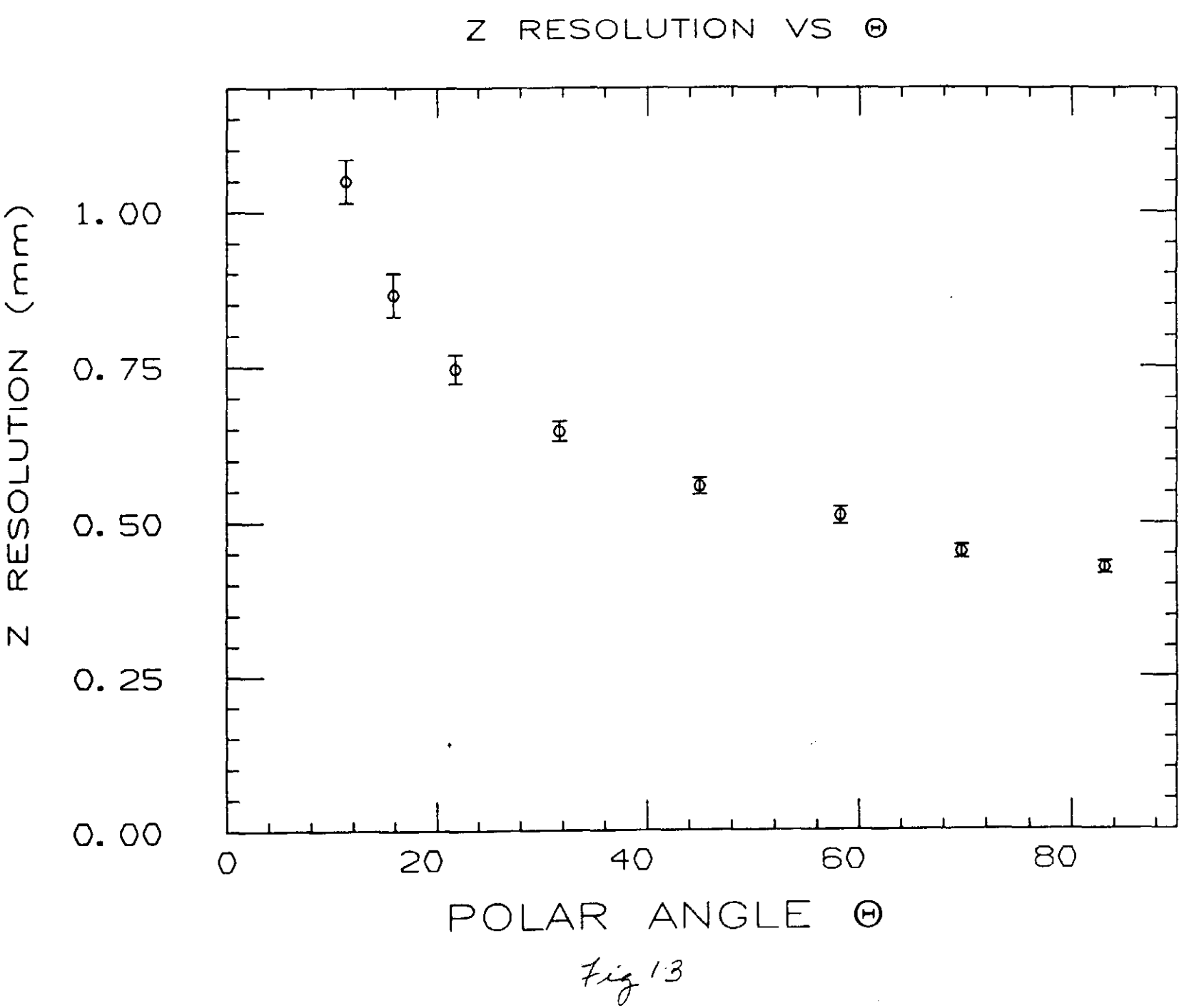
Z RESOLUTION VS Θ
Z RESOLUTION (mm)
1.00
0.75
0.50
0.25
0.00
0
20
40
60
80
POLAR ANGLE Θ

Fig 13

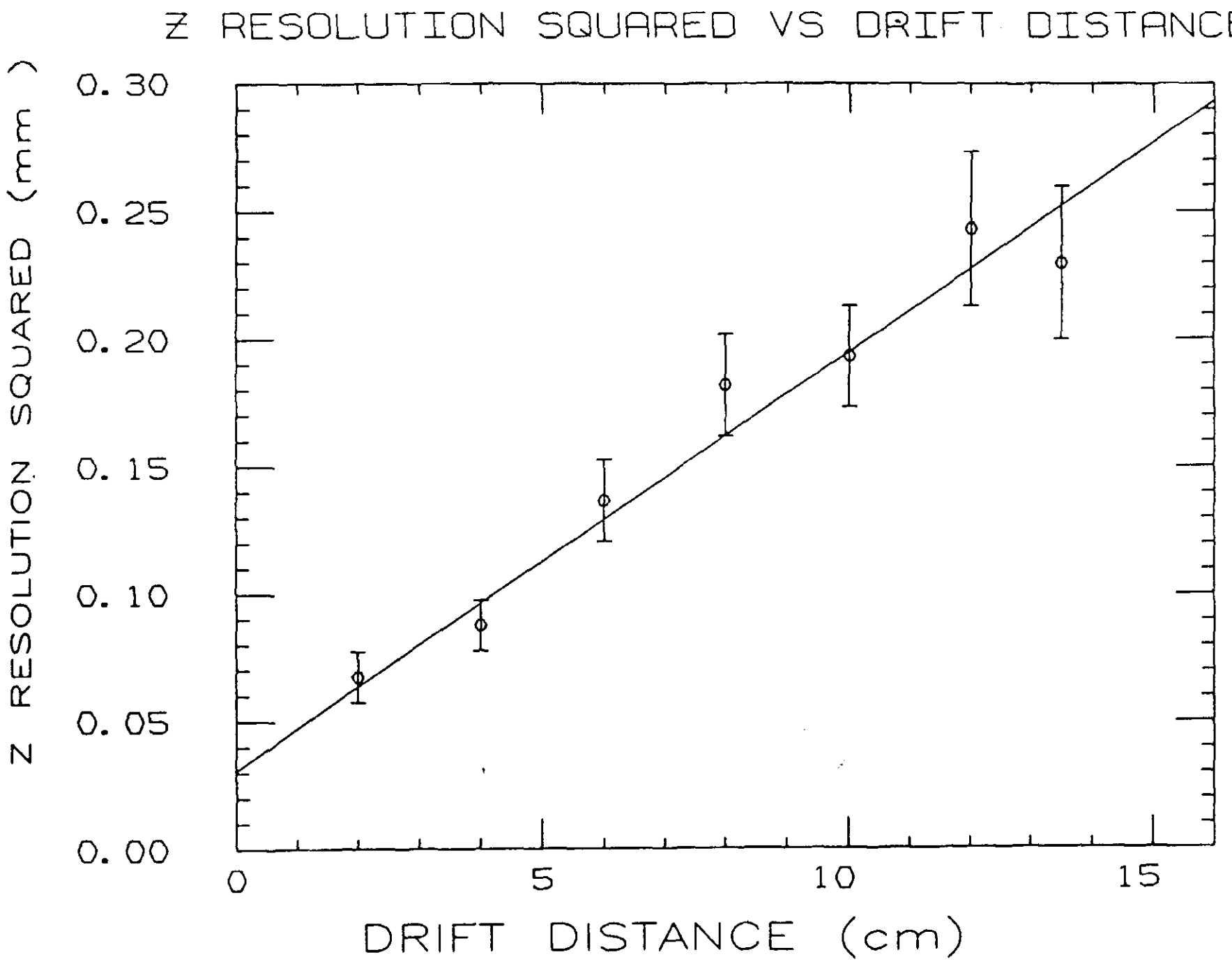
Z RESOLUTION SQUARED VS DRIFT DISTANCE
Z RESOLUTION SQUARED (mm)
0.30
0.25
0.20
0.15
0.10
0.05
0.00
0
5
10
15
DRIFT DISTANCE (cm)

Fig 14

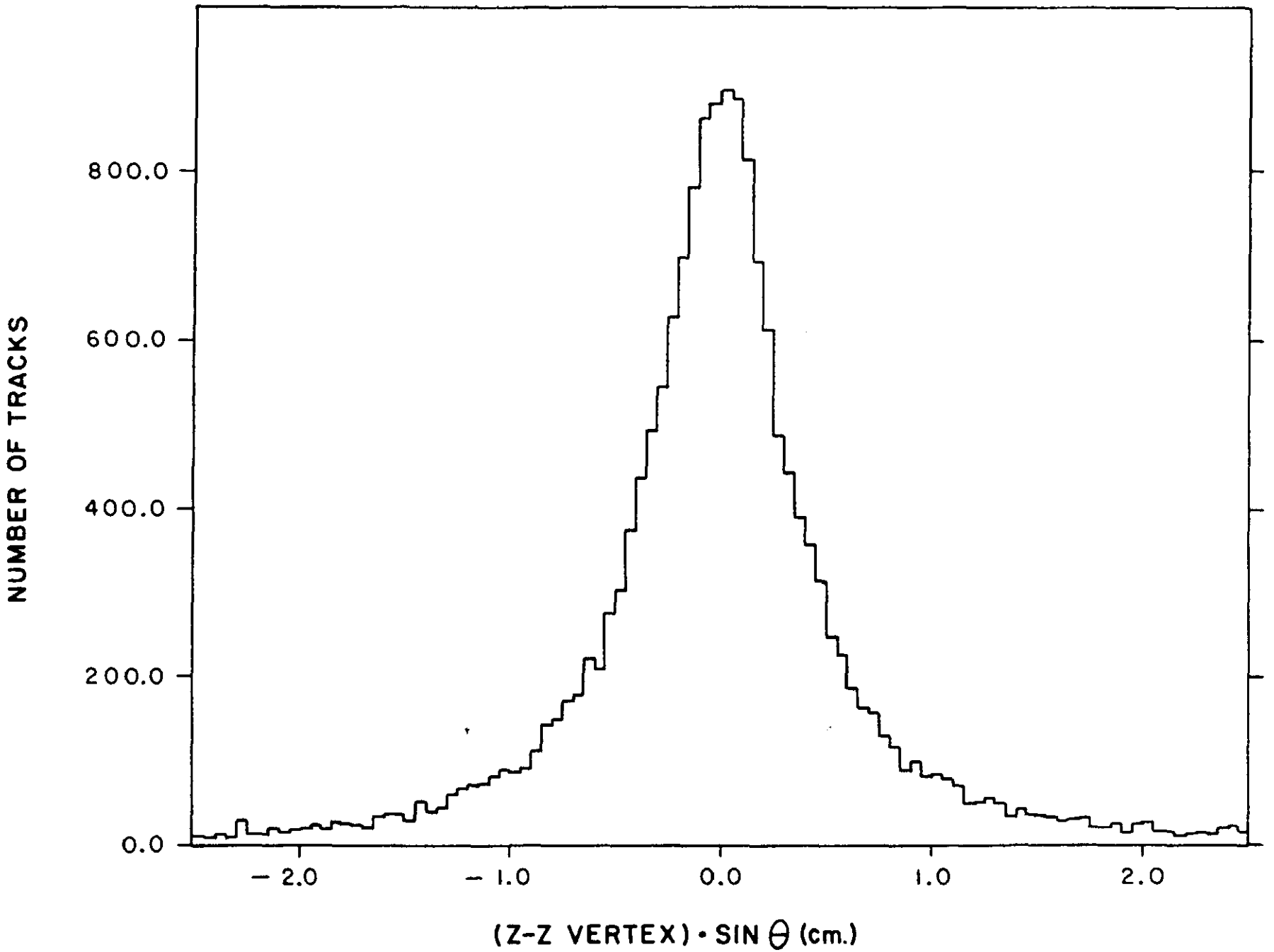
NUMBER OF TRACKS
800.0
600.0
400.0
200.0
0.0
− 2.0
− 1.0
0.0
1.0
2.0
(Z-Z VERTEX) • SIN θ (cm.)

Fig 15

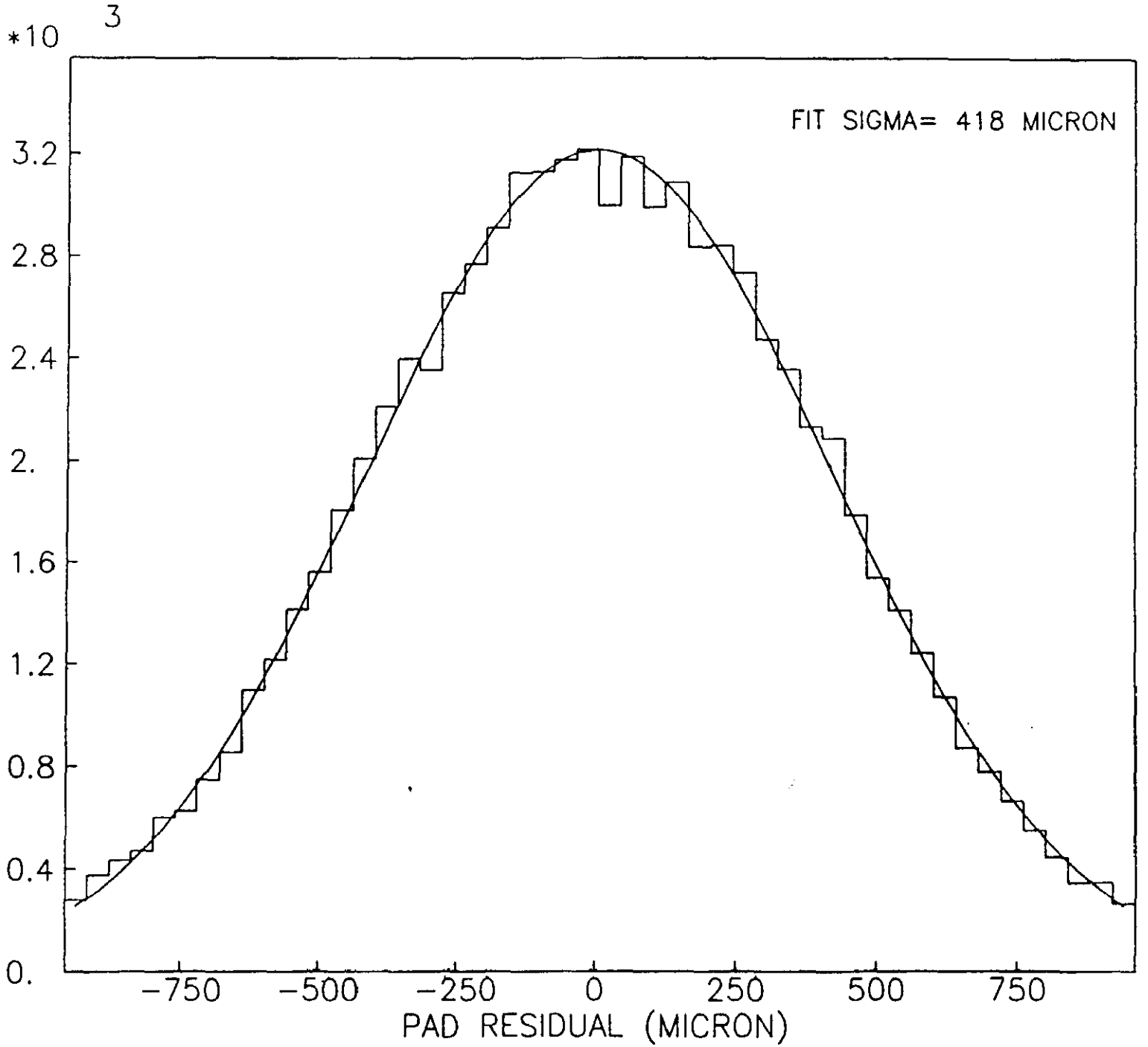
*10 3
FIT SIGMA= 418 MICRON
3.2
2.8
2.4
2.
1.6
1.2
0.8
0.4
0.
-750
-500
-250
0
250
500
750
PAD RESIDUAL (MICRON)

Fig 16